Neutron Star Binaries at $1064\ \mathrm{nm}$

Matthias U. Kruckow

collaborators: T. M. Tauris, N. Langer, ...

Argelander-Institut für Astronomie
Rheinischen Friedrich-Wilhelms-Universität Bonn

12^{th} December 2017

XI. BONN NS workshop

Argelander-Institut für Astronomie

UNIVERSITÄT BONN

Laser and Optics

- $4\ \mathrm{W}$ laser at $808\ \mathrm{nm}$ is converted to $1064\ \mathrm{nm}$ with a power of $2\ \mathrm{W}$ and then amplified to $200\ \mathrm{W}$ before the beam enters the interferometer
- Split the beam in two perpendicular arms
- Try to detect a change in distance between its mirrors of $10^{-19}\ \mathrm{m}$ about $\frac{1}{10\,000}$ the width of a proton

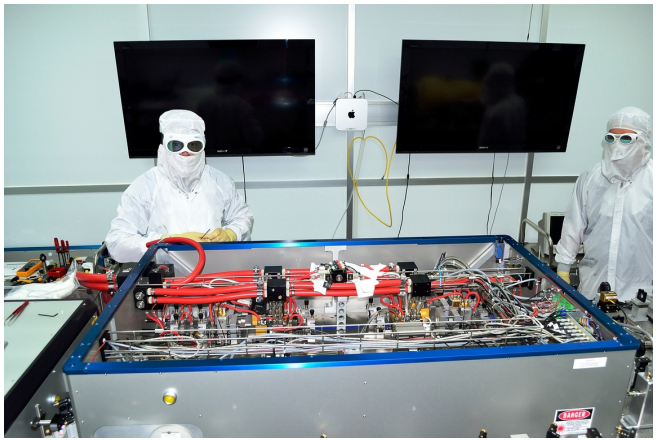

laser during maintenance

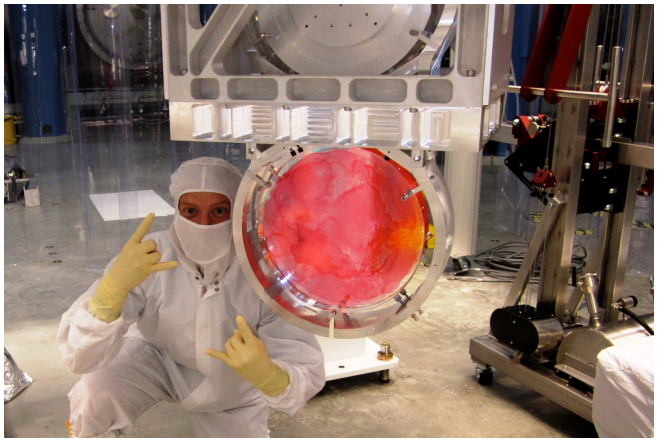

beam splitter

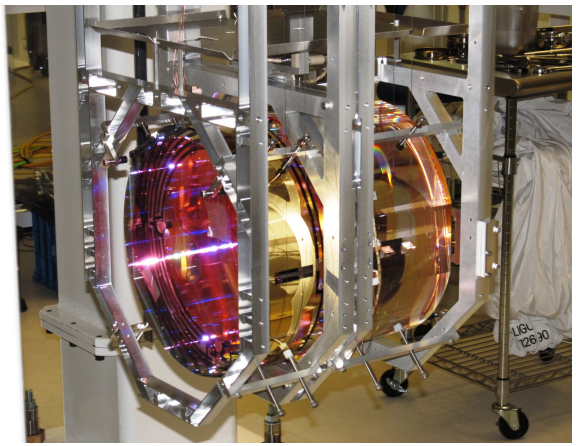

test mass with mirror
credits: LIGO

Two Observatories in USA

- $4\,\mathrm{km}$ arm length
- vacuum chamber volume of $10\,000\,\mathrm{m}^3$ with air pressure of $10^{-9}\,\mathrm{Torr} \approx 10^{-12}\,\mathrm{atm}$

Hanford Observatory

Livingston Observatory

credits: LIGO

The Observatory in Italy

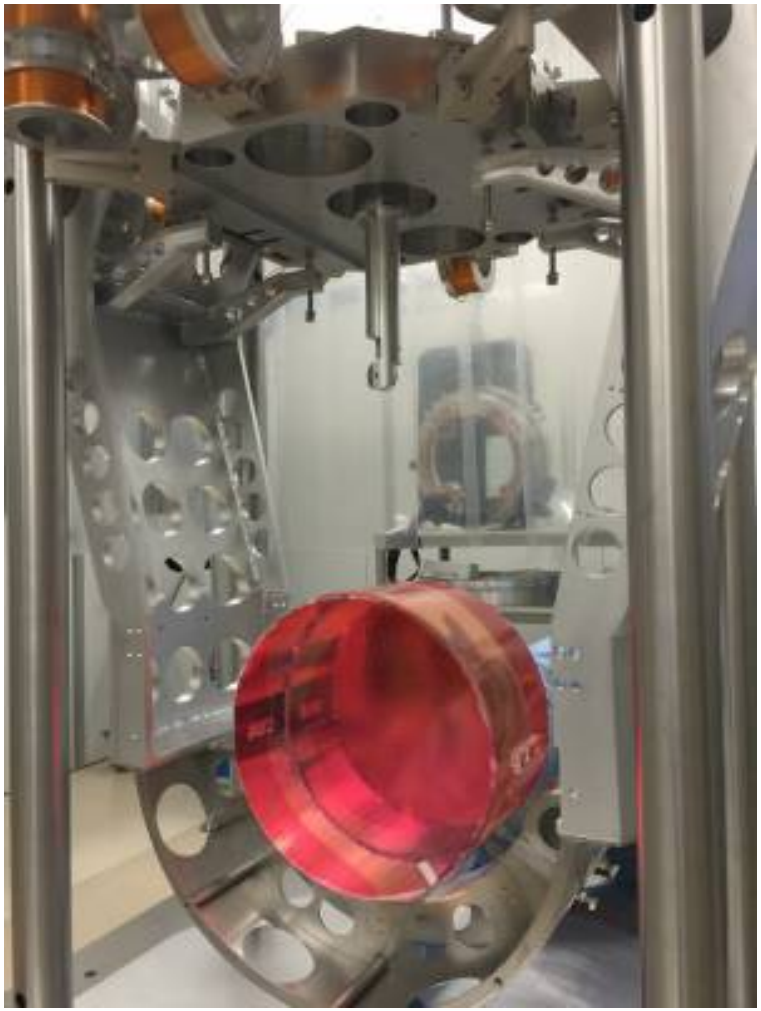

$42\ \mathrm{kg}$ mirror

- $3\ \mathrm{km}$ arm length

Virgo Observatory

credits: Virgo Collaboration

Outline

1. Gravitational Wave Detectors
2. Binary Population Synthesis
3. Double Neutron Star Binaries
4. Gravitational Wave Mergers
5. Summary

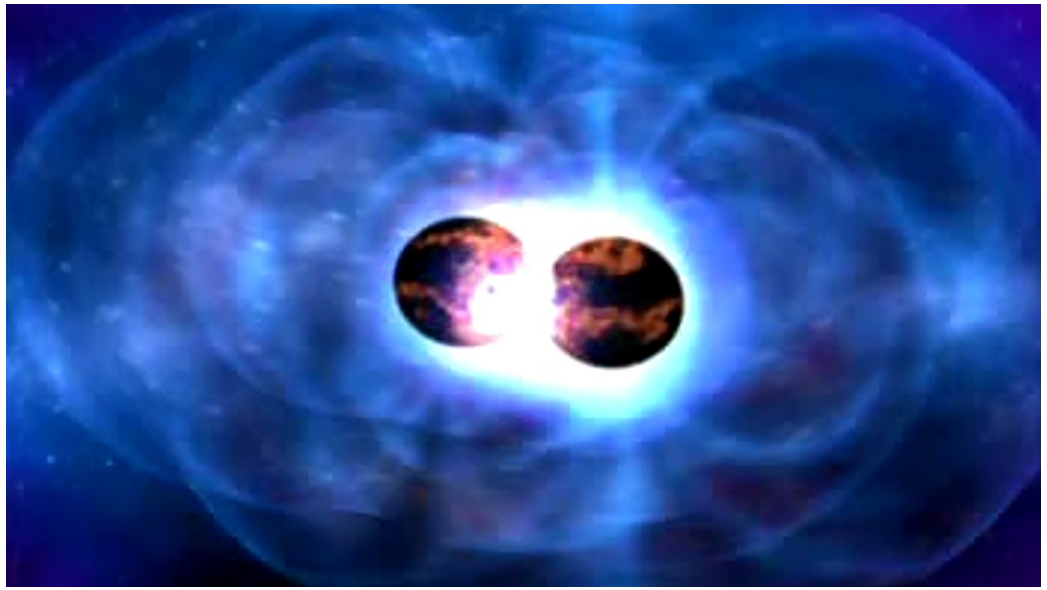

Two merging neutron stars

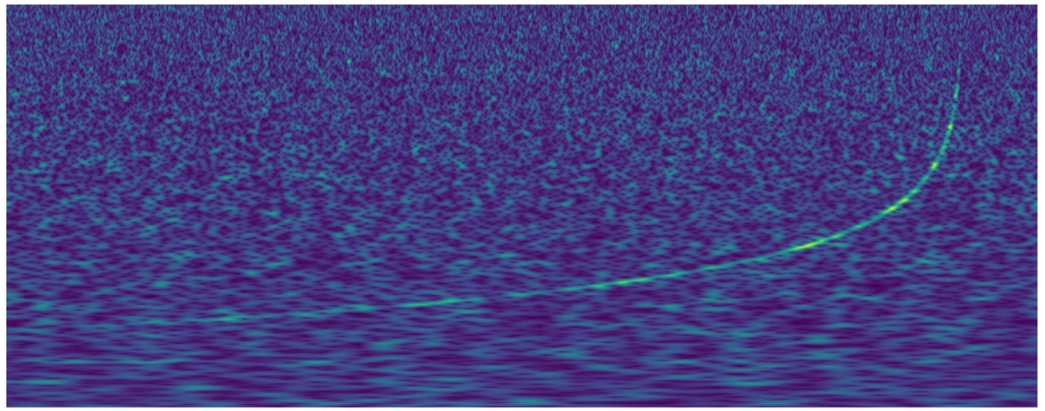

Gravitational wave chirp spectrogram

credits: LIGO

Overview

- Aim: fast evolution of a large sample of binaries

→ Get general trends/relations of populations in star clusters or galaxies i.e. merger rates of compact object binaries (e.g. Clark et al. 1979)

- Several binary population synthesis codes
  - ComBinE (Kruckow et al. 2018, submitted to MNRAS)
  - StarTrack (Belczynski et al. 2008; Dominik et al. 2013, 2015; Chruslinska et al. 2017)
  - binary_c (Izzard et al. 2004, 2006, 2009, 2017)
  - BPASS (Eldridge & Stanway 2016; Eldridge et al. 2017)
  - COMPAS (Stevenson et al. 2017; Barrett et al. 2017)
  - MOBSE (Mapelli et al. 2017; Giacobbo et al. 2017)
  - others

Binary Evolution

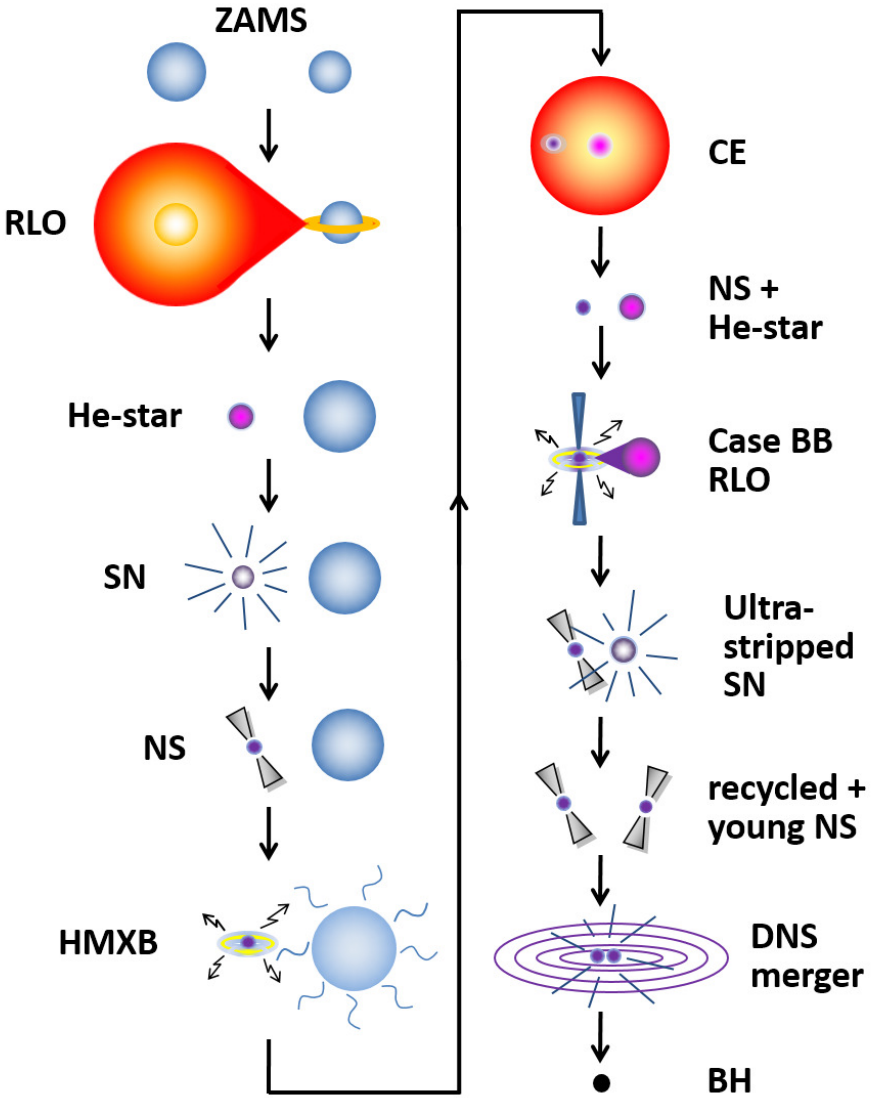

- Initial conditions at ZAMS
- Stellar evolution from interpolated grids
- Stable Roche-lobe overflow (RLO)
- He-star evolution from interpolated grids
- Supernova (SN) treatment
- Common envelope (CE) phase
- Ultra-stripped SN treatment
- Gravitational wave radiation

Tauris et al. (2017)

Interpolate Stellar Grids

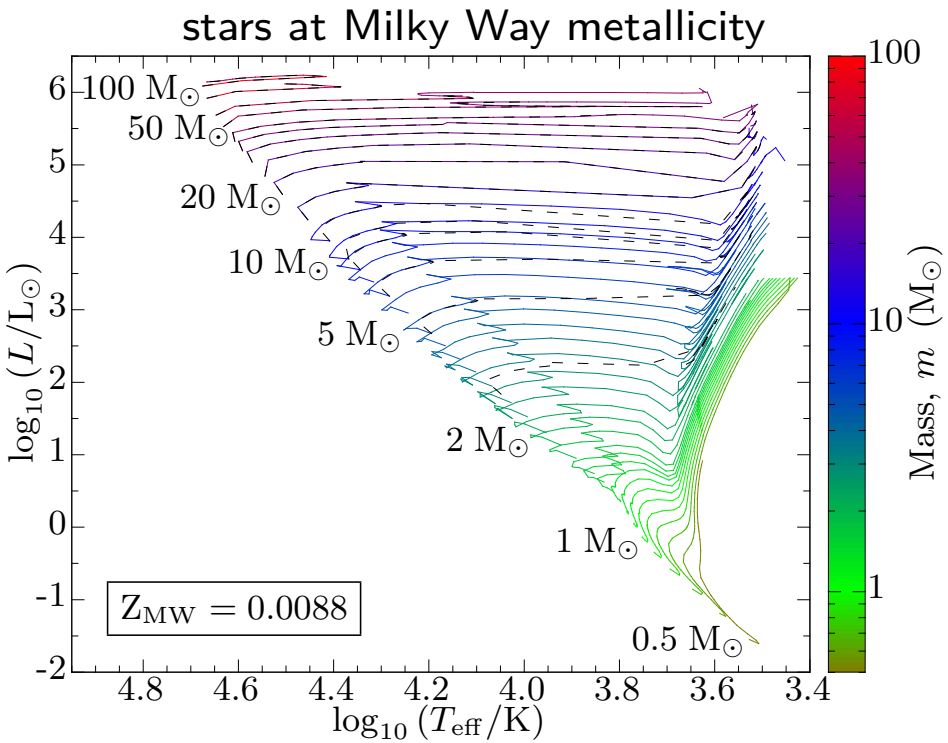

- Fast stellar evolution

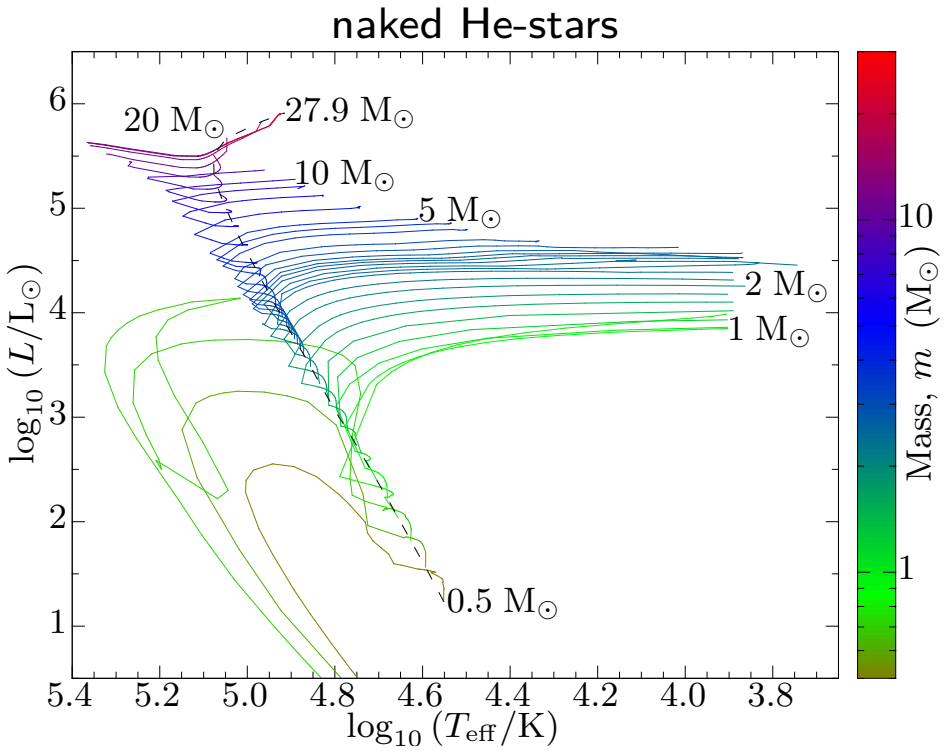

- Quickly and easily add/update stellar evolution

Kruckow et al. (2018)

Common Envelope – In-spiral

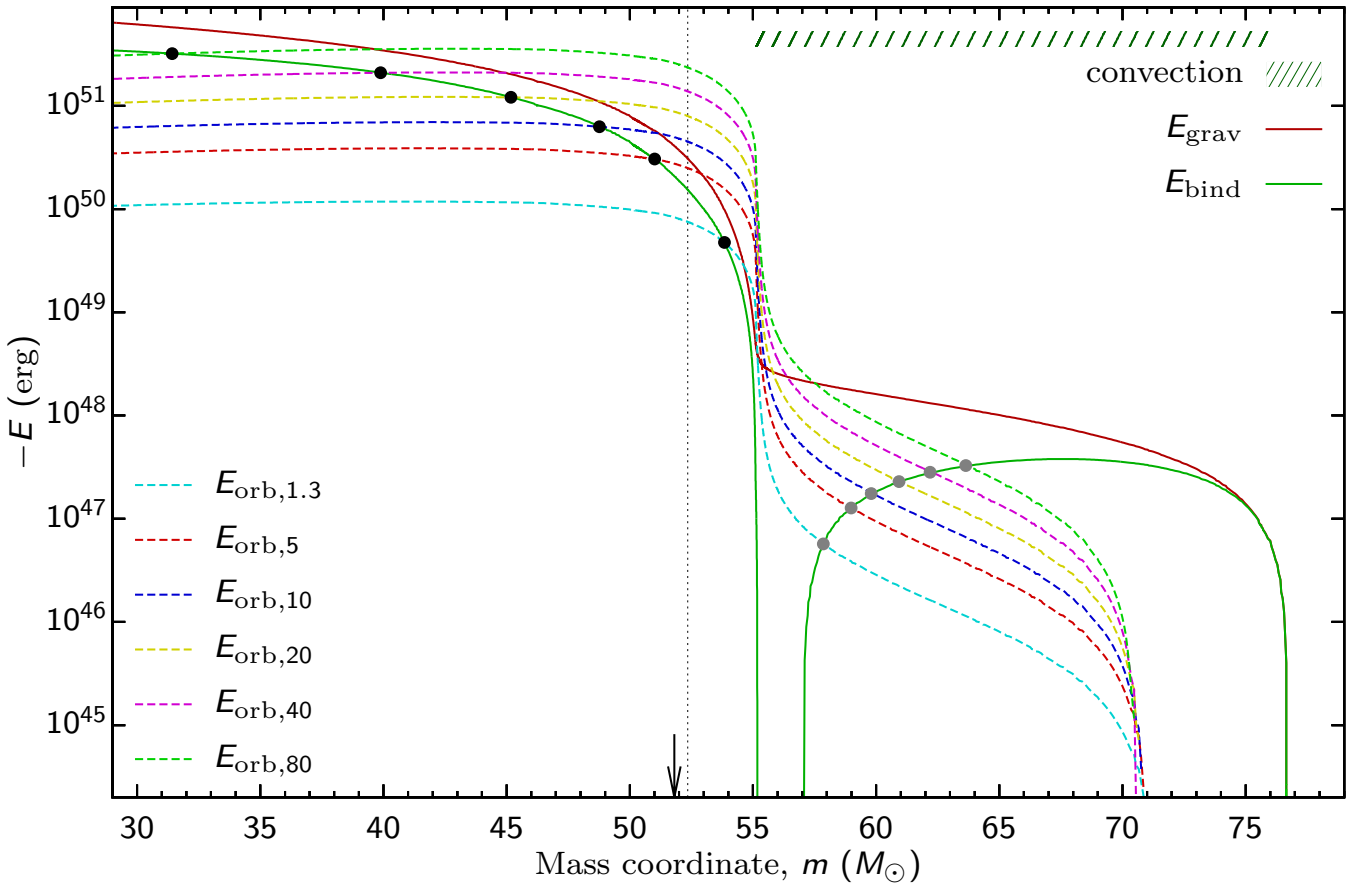

initial star
$m_{\rm ZAMS}$=88 $\rm M_\odot$
Z=0.0002

as giant (left plot)
m=76.65 $\rm M_\odot$
R=3530 $\rm R_\odot$
$m_{\rm core}$=52.35 $\rm M_\odot$

Kruckow et al. (2016)

- Where does the in-spiral stop?

→ Large uncertainties

Common Envelope – In-spiral

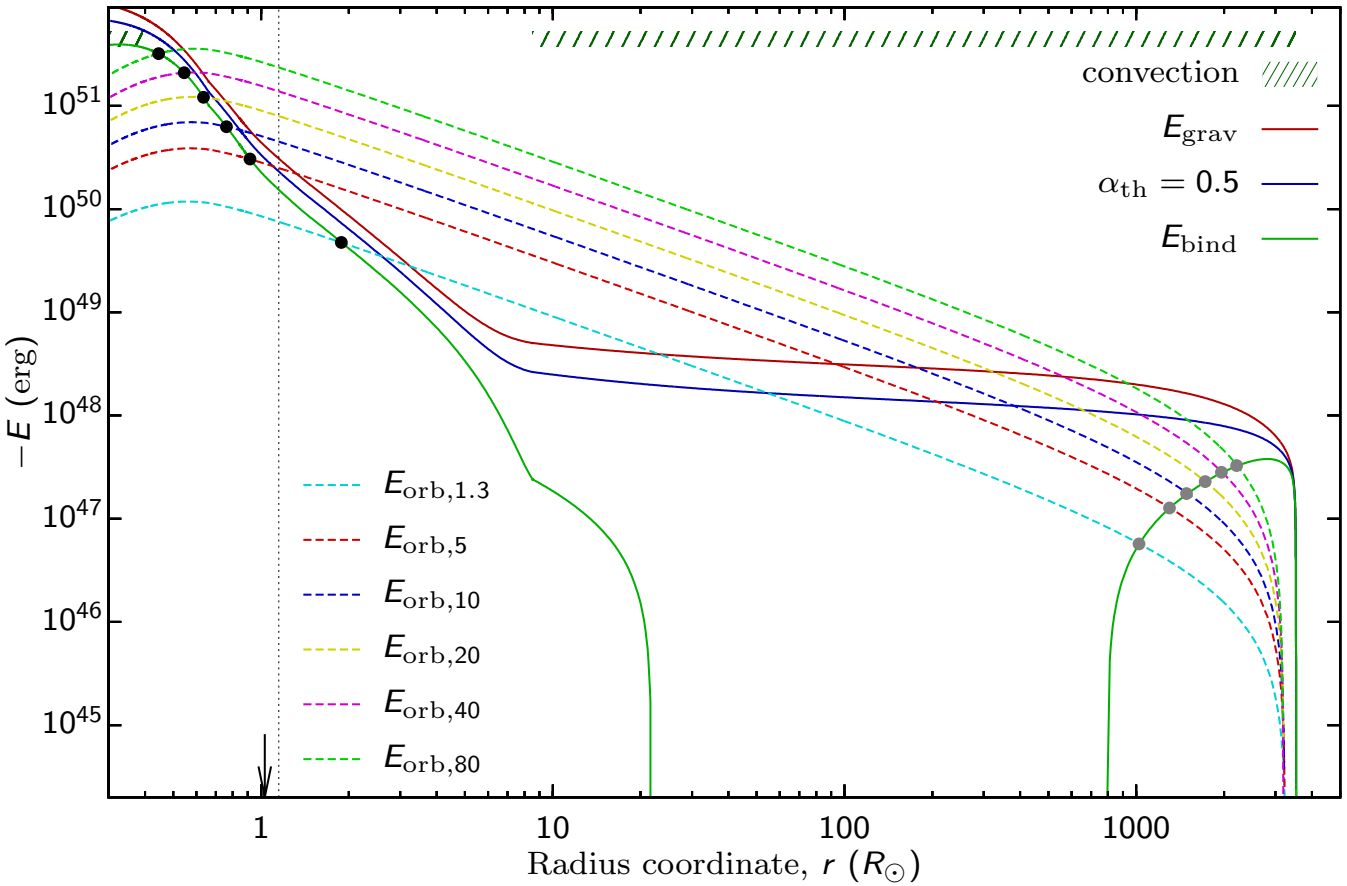

initial star

$m_{\rm ZAMS}$=88 $\rm M_\odot$

Z=0.0002

as giant (left plot)

m=76.65 $\rm M_\odot$

R=3530 $\rm R_\odot$

$m_{\rm core}$=52.35 $\rm M_\odot$

Kruckow et al. (2016)

- Where does the in-spiral stop?

→ Large uncertainties

Supernova Kicks

- Asymmetries in the ejected material lead to kicks
  - Disrupt binary → hyper-velocity stars
  - Eccentric binaries → larger GW emission
- Exploding shell impacts on the companion (Liu et al. 2015)
- Ultra stripped SN (Tauris et al. 2015)

Table 1. Projected 1-dimensional root-mean-square kick velocity values $\left(w_{\rm rms}^{\rm 1D}\right)$ or 3-dimensional kick velocity ranges, applied to various exploding stars.

SN type	first SN	second SN
Electron capture SN *	0 – 50 km s^{-1}	0 – 50 km s^{-1}
Iron-core collapse SN depending on the NS progenitor:		
– Isolated star or wide binary	265 km s^{-1}	265 km s^{-1}
– Close binary, no H-env. **	120 km s^{-1}	120 km s^{-1}
– Close binary, no He-env. **	60 km s^{-1}	30 km s^{-1}
Formation of BH *	0 – 200 km s^{-1}	0 – 200 km s^{-1}

* Here, the stated velocity interval corresponds to 3-dimensional velocities and we applied a flat probability distribution rather than applying a Maxwellian distribution.
** For iron-core collapse SNe in close systems, we applied a bimodal kick distribution such that the above $w_{\rm rms}^{\rm 1D}$ values for a Maxwellian distribution account for 80 per cent of the cases and in the remaining 20 per cent of the cases we applied a larger kick using $w_{\rm rms}^{\rm 1D} = 200$ km s^{-1} (see section 2.2.6).

Kruckow et al. (2018)

Primary and Secondary Mass at MW-like Metallicity

- Highly inefficient mass transfer needed
- Are there too many electron capture SNe in the sample, becaused assumed small SN kicks
  or is the mass of a NS from an ECSN $\sim 0.08\ \mathrm{M}_\odot$ larger than expected?

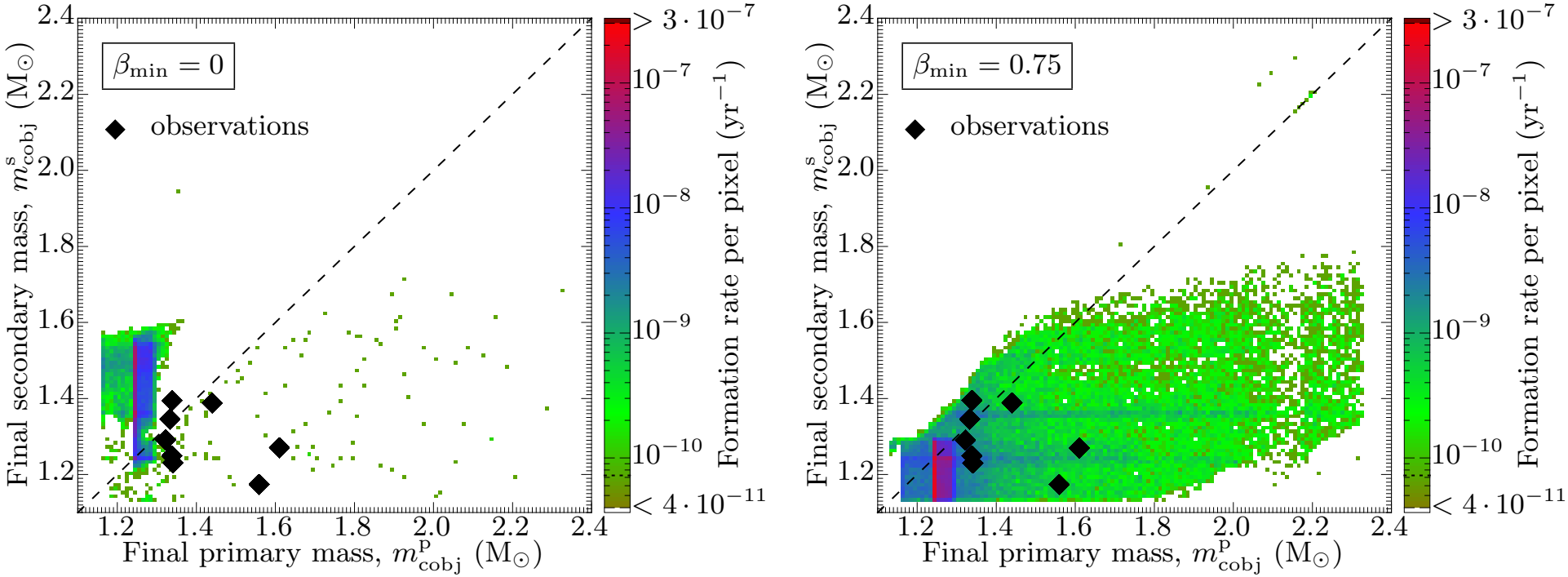

Kruckow et al. (2018)

Mass Ratios at MW-like Metallicity

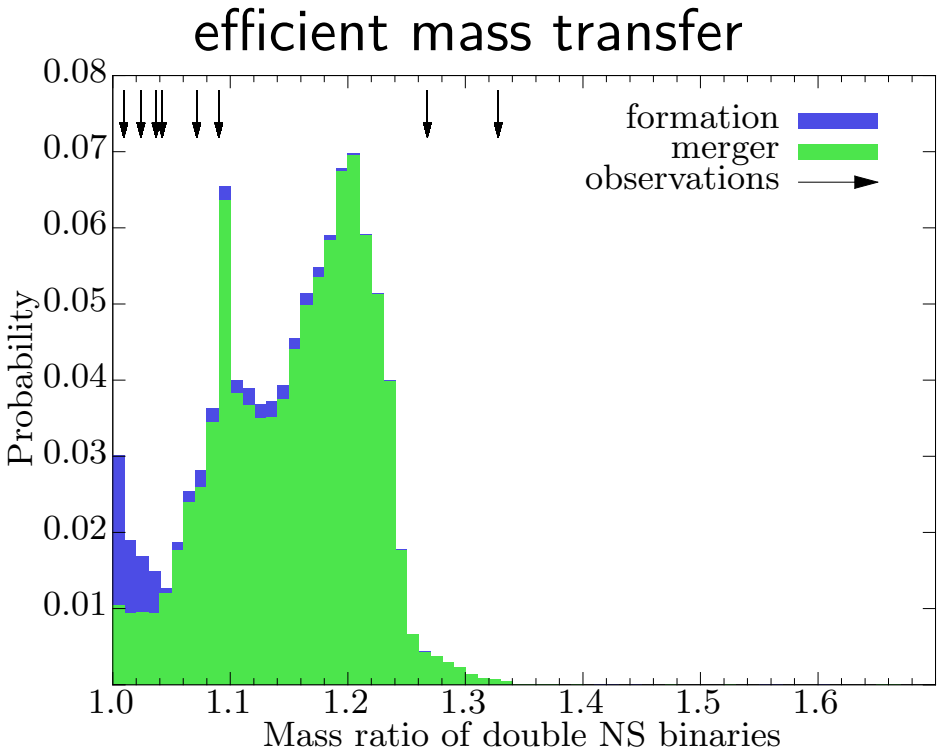

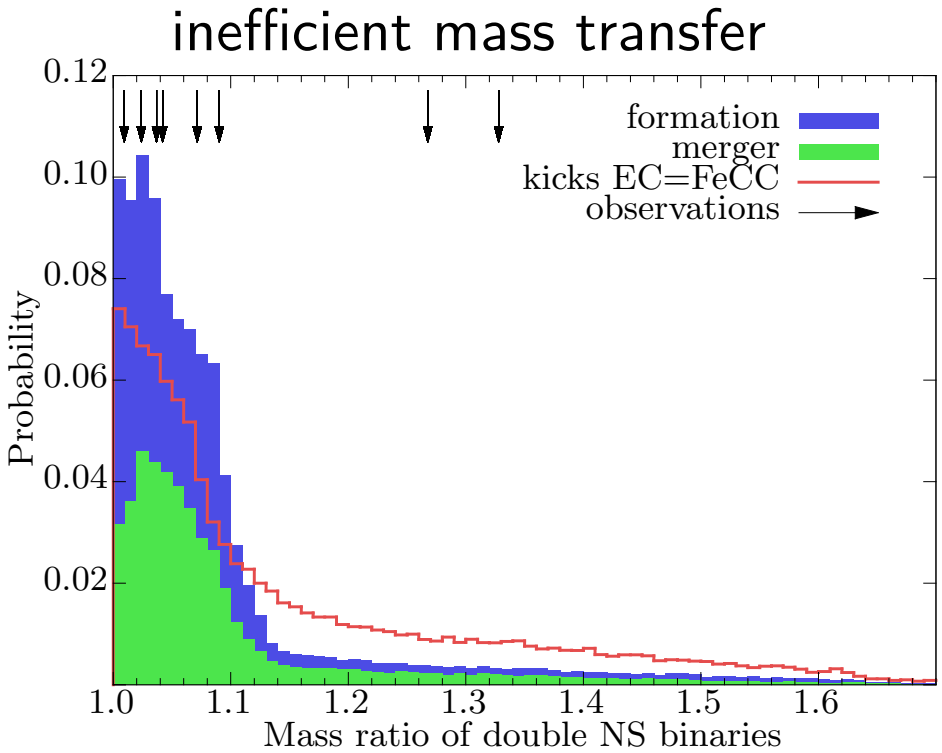

Kruckow et al. (2018)

- Highly inefficient mass transfer needed

→ Match with observations

Orbital Parameters

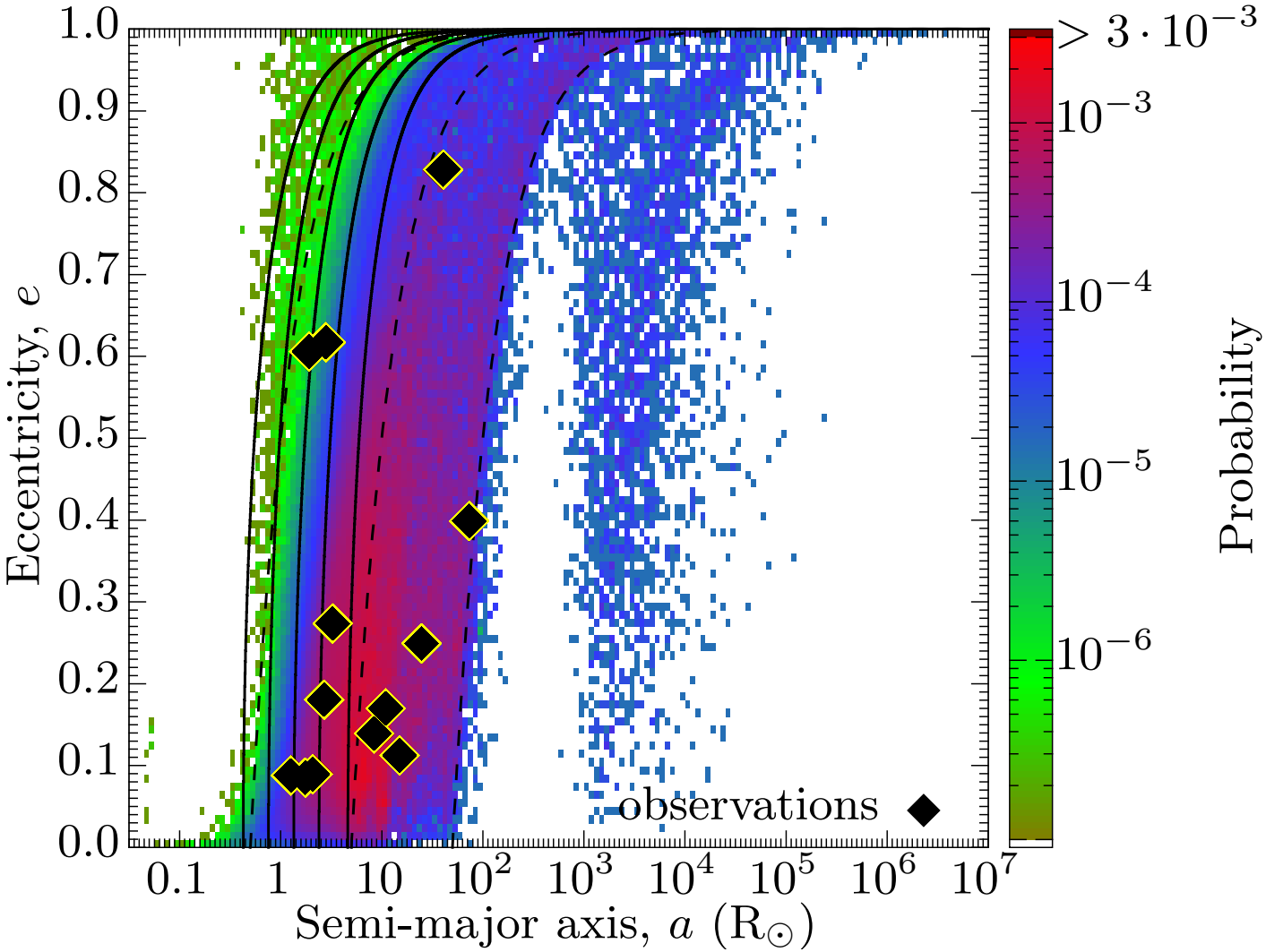

- Separated regions for binaries with and without CE evolution
- Observed double NS binaries agree well with our population synthesis results

Kruckow et al. (2018)

Systems in the MW Galaxy

Table 7. Number of DCO systems present in the Milky Way as a function of the parameter $\beta_{\rm min}$, where the maximum RLO mass-transfer efficiency is given by $\epsilon_{\rm max} = 1 - \alpha_{\rm RLO} - \beta_{\rm min}$. The numbers are given for stellar evolution lasting (10 ± 3.81) Gyr. The binary types indicate the order of the first and second-formed compact objects.

Systems in MW	$\beta_{\rm min} = 0.75$	$\beta_{\rm min} = 0.5$	$\beta_{\rm min} = 0$
NS-NS	38246^{+12445}_{-13100}	41340^{+12624}_{-13405}	1616^{+499}_{-505}
NS-BH	55^{+21}_{-21}	19^{+7}_{-7}	25^{+9}_{-10}
BH-NS	108845^{+36702}_{-37811}	21303^{+7504}_{-7687}	13603^{+4532}_{-4798}
BH-BH	20073^{+7585}_{-7602}	16237^{+5934}_{-6006}	21988^{+8247}_{-8267}

Kruckow et al. (2018)

- Lower limit of first born pulsars' active radio lifetime of about $100\ \mathrm{Myr}$

$\rightarrow$ at least 400 active radio pulsars in double NS systems in the MW

- Low chance of finding a recycled pulsar orbiting a BH

The Seven LIGO Detections

- Until August 2017 only BH mergers detected

- GW170817
  $\mathcal{M} = 1.188^{+0.004}_{-0.002}\ \mathrm{M}_\odot$
  $M = 2.74^{+0.04}_{-0.01}\ \mathrm{M}_\odot$

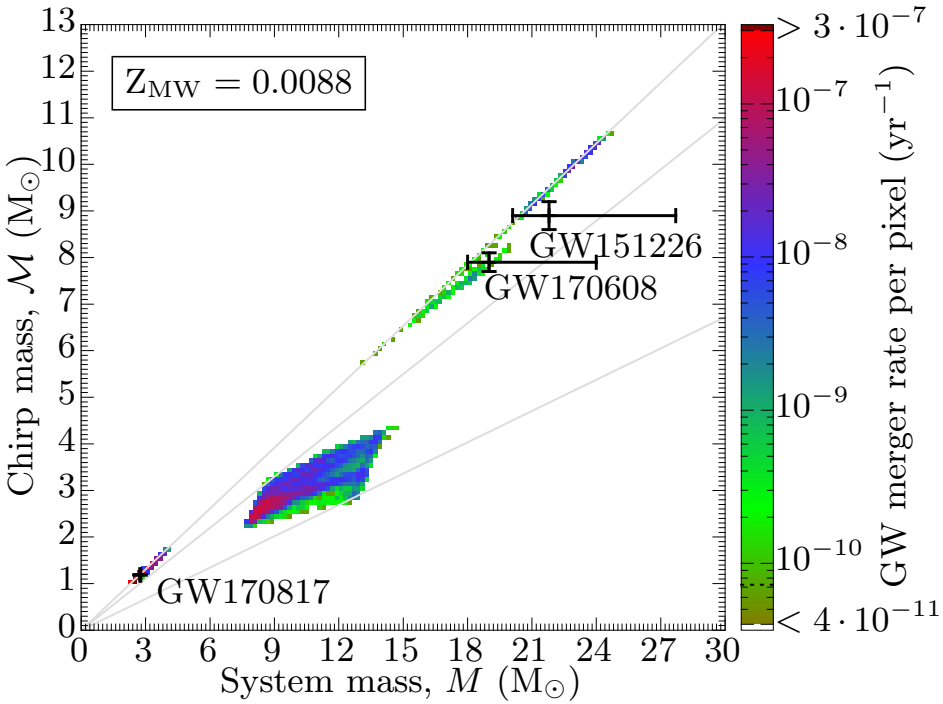

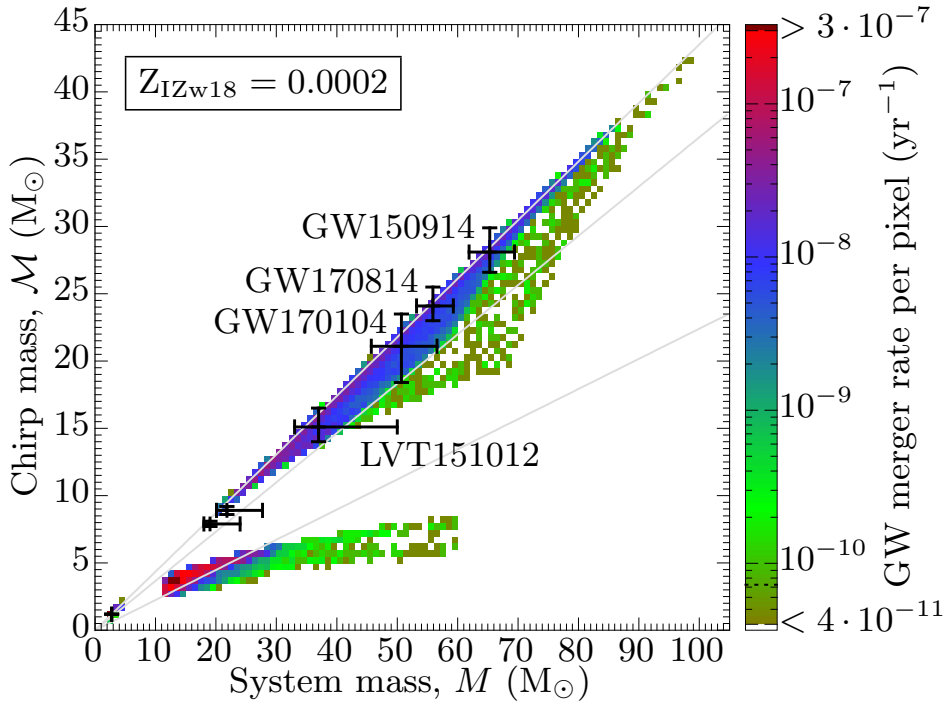

Kruckow et al. (2018)

Neutron Star Mergers (most recent works)

- Constrain equation of state for NSs on in-spiral (e.g. Rezzolla et al. 2017; Ruiz et al. 2017; Annala et al. 2017; Tiziano et al. 2017)

- Joint observations of GW (several papers of Abbott et al. 2017) and electromagnetic spectrum (e.g. Soares-Santos et al. 2017; Hallinan et al. 2017; Shappee et al. 2017)
  - Get properties of short GRBs like beaming angle (e.g. Yamaski et al. 2017; Tong & Yu 2017; Mooley et al. 2017; Williams et al. 2017)
  - Ejecta $\rightarrow$ enrichment of their environment in heavy elements (e.g. Kasen et al. 2017; Pian et al. 2017; Thielemann et al. 2017; Asano & To 2017; Waxman et al. 2017)
  - Remnant: NS, BH, something else (e.g. Chatziioannou et al. 2017; Ma et al. 2017; Pooley et al. 2017)
  - Delay times between GW and EM signal constrain gravity theories (e.g. Boran et al. 2017)

GW170817 and GRB170817A

- Host galaxy identified as NGC 4993 (e.g. Soares-Santos et al. 2017; Coulter et al. 2017)
  - S0 galaxy
  - about $40\ \mathrm{Mpc}$ away
  - metallicity between 0.2 and $1.0\ \mathrm{Z}_\odot$ (e.g. Im et al. 2017)
  - $M \approx 10^{10.5}\ \mathrm{M}_\odot$ (e.g. Pan et al. 2017)

- GRB170817A located within the effective radius of NGC 4993 (e.g. Blanchard et al. 2017)

→ bound to NGC 4993 implies that systemic velocity of the double NS binary is probably below $350\ \mathrm{km/s}$

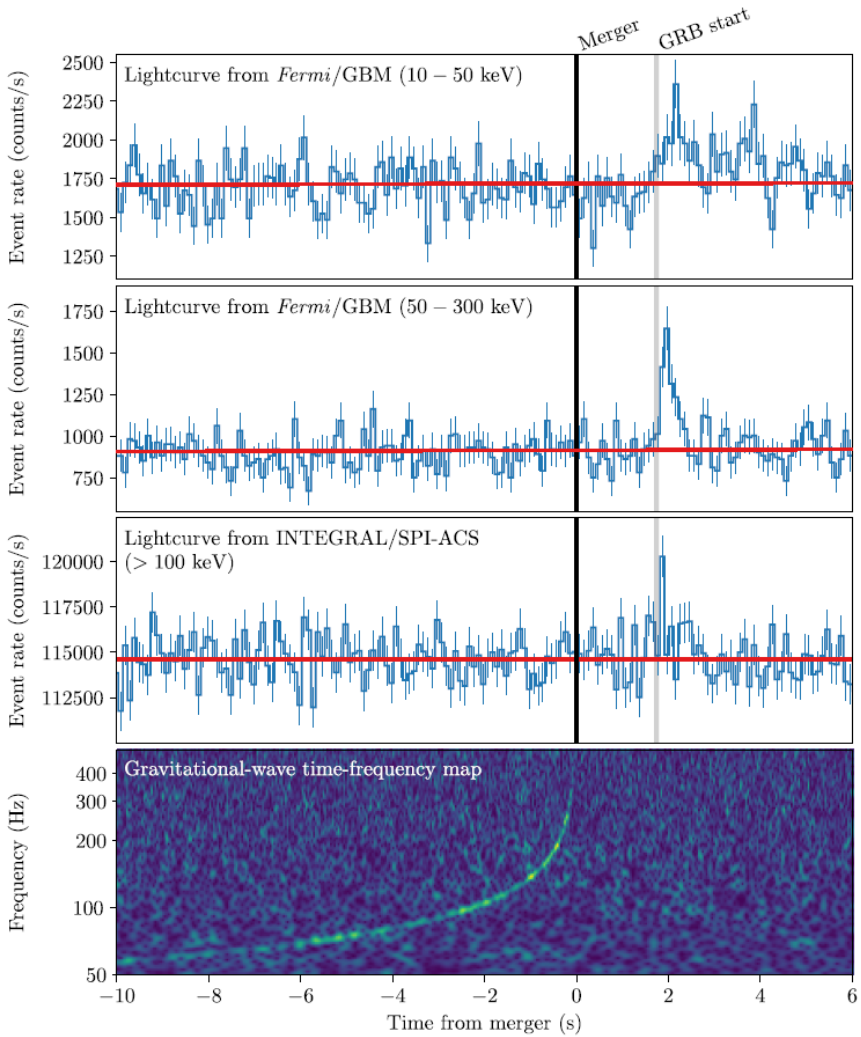

Figure 2. Joint, multi-messenger detection of GW170817 and GRB 170817A. Top: the summed GBM lightcurve for sodium iodide (NaI) detectors 1, 2, and 5 for GRB 170817A between 10 and 50 keV, matching the 100 ms time bins of the SPI-ACS data. The background estimate from Goldstein et al. (2016) is overlaid in red. Second: the same as the top panel but in the 50–300 keV energy range. Third: the SPI-ACS lightcurve with the energy range starting approximately at 100 keV and with a high energy limit of least 80 MeV. Bottom: the time-frequency map of GW170817 was obtained by coherently combining LIGO-Hanford and LIGO-Livingston data. All times here are referenced to the GW170817 trigger time T_0^{GW}.

Abbott et al. (2017)

Progenitors of GW170817

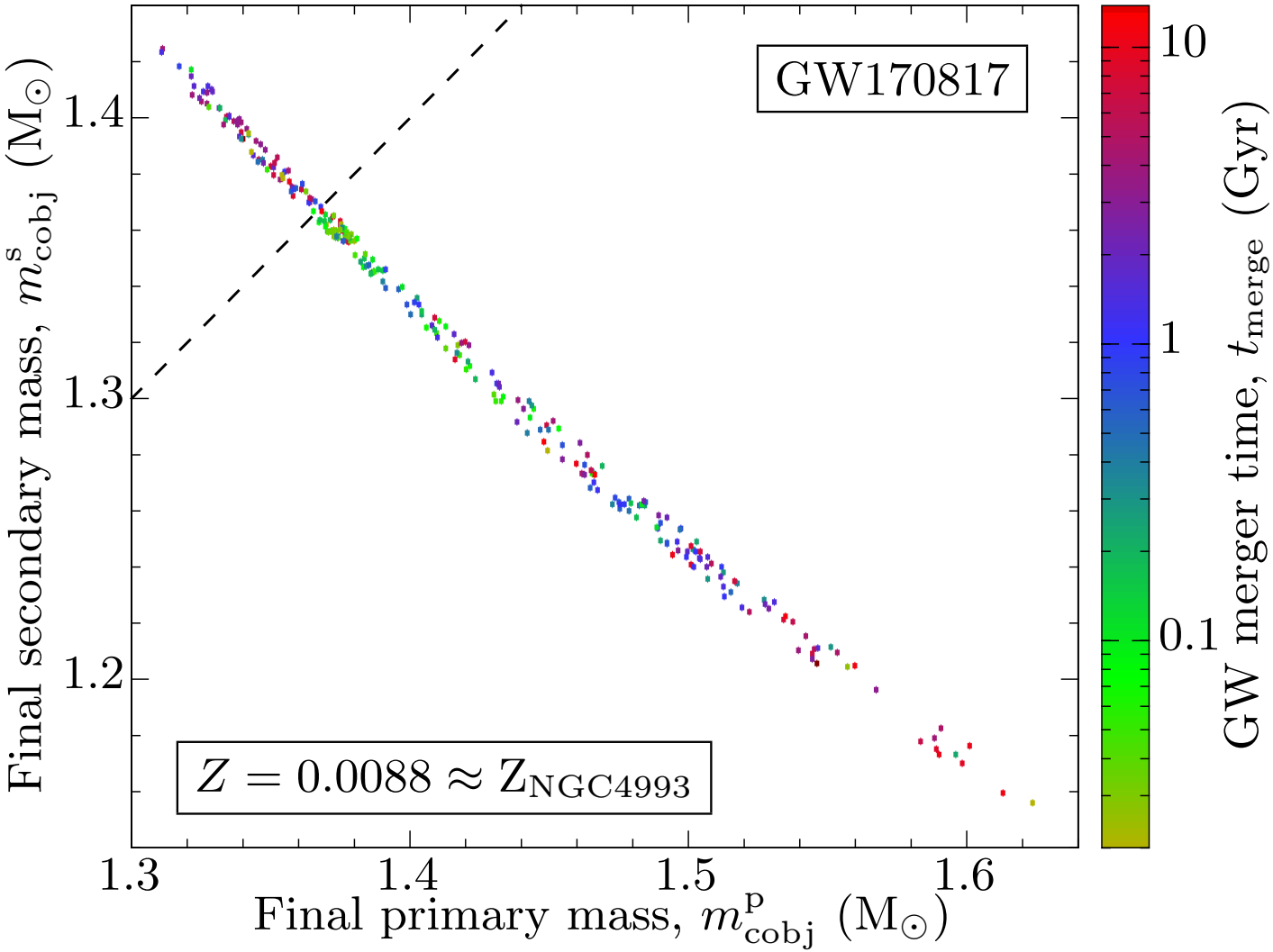

Kruckow et al. (2018)

- negligible recent star formation in NGC 4993 (e.g. Pan et al. 2017)

→ progenitor system at least a few Gyr old

- several possible formation scenarios (Belczynski et al. 2017)

Progenitors of all Seven LIGO Mergers

- All seven reported LIGO events are reproduced depending on metallicity

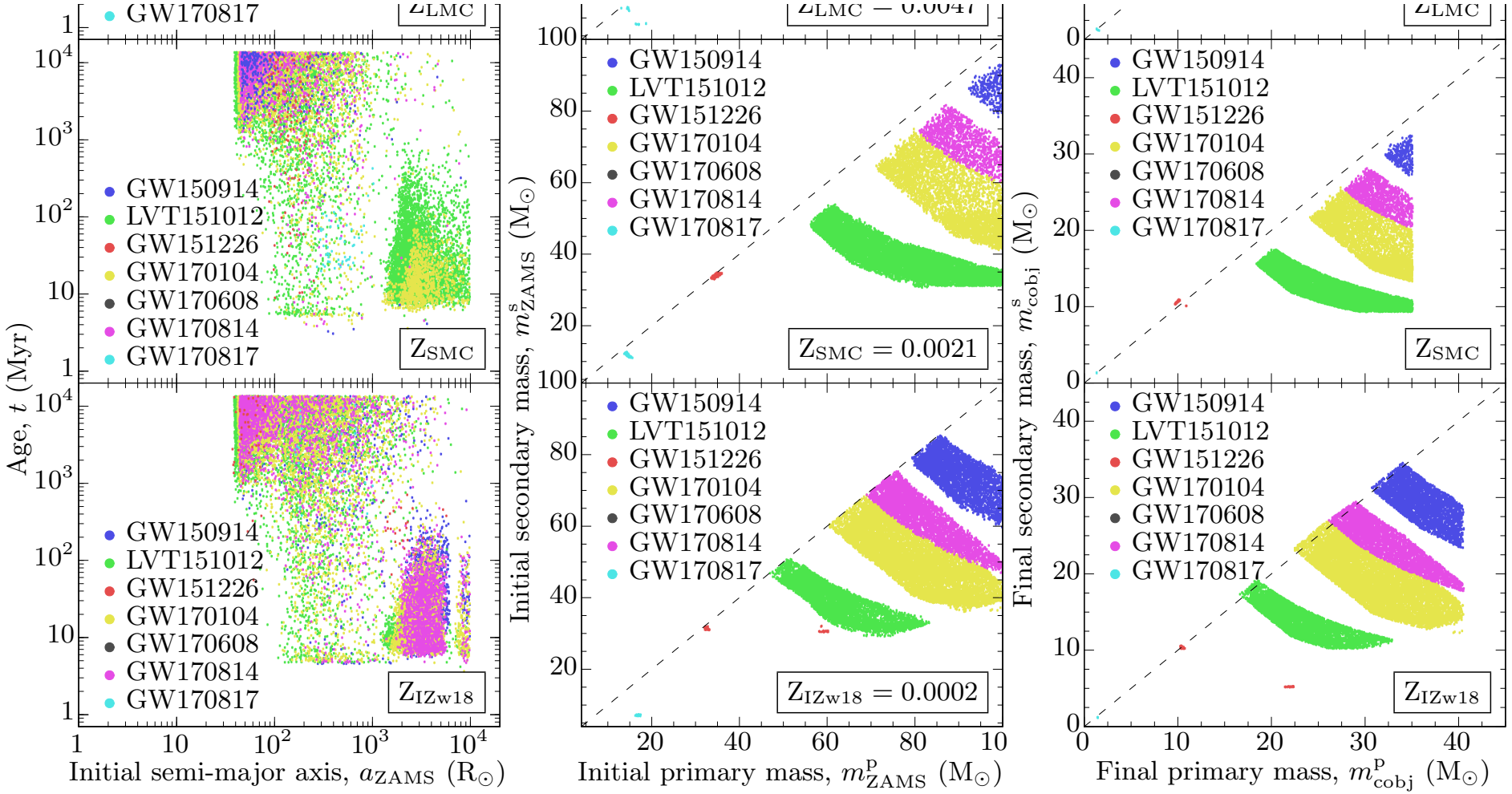

Kruckow et al. (2018)

Progenitors of all Seven LIGO Mergers

- All seven reported LIGO events are reproduced depending on metallicity

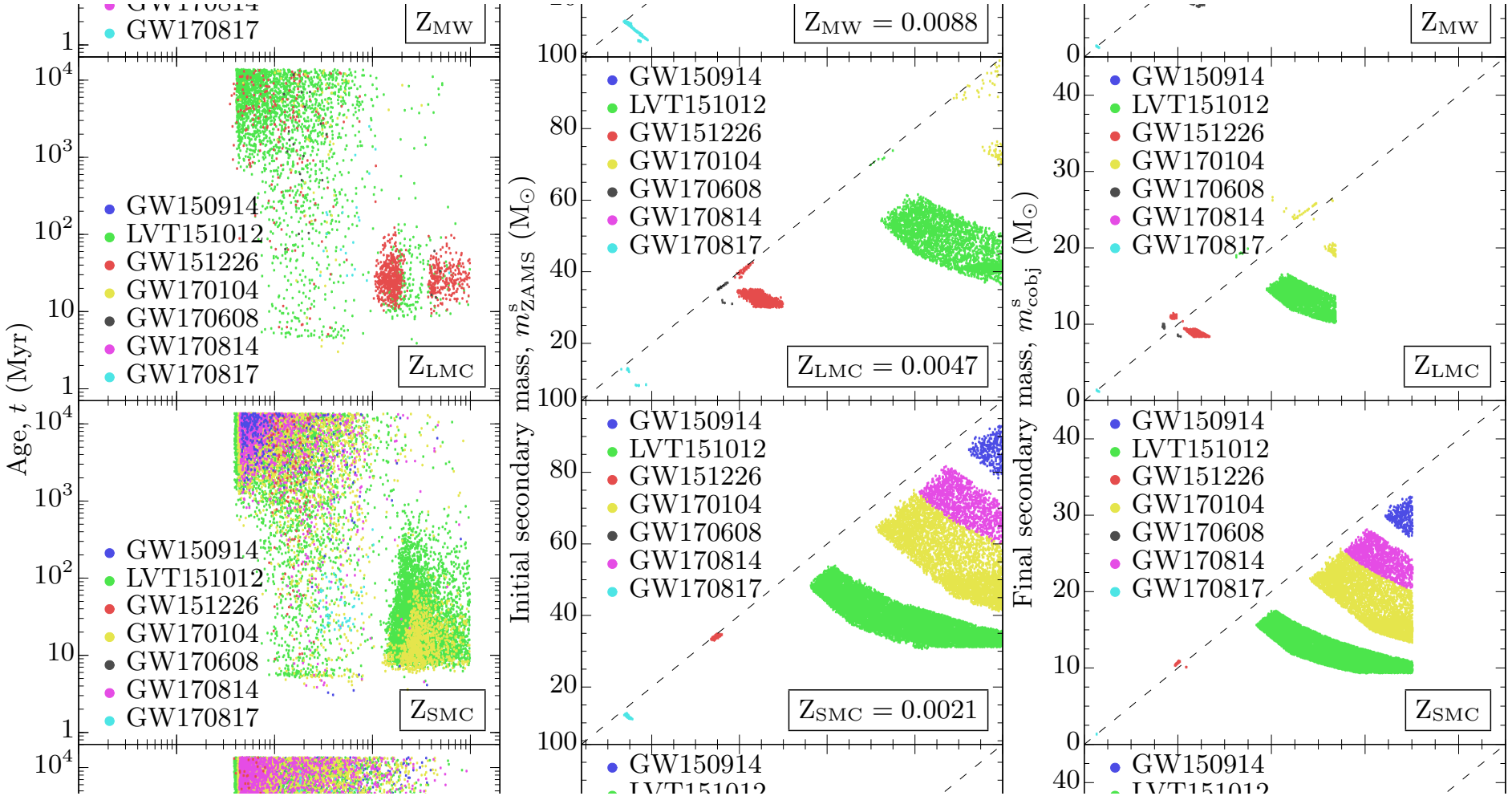

Kruckow et al. (2018)

Progenitors of all Seven LIGO Mergers

- All seven reported LIGO events are reproduced depending on metallicity

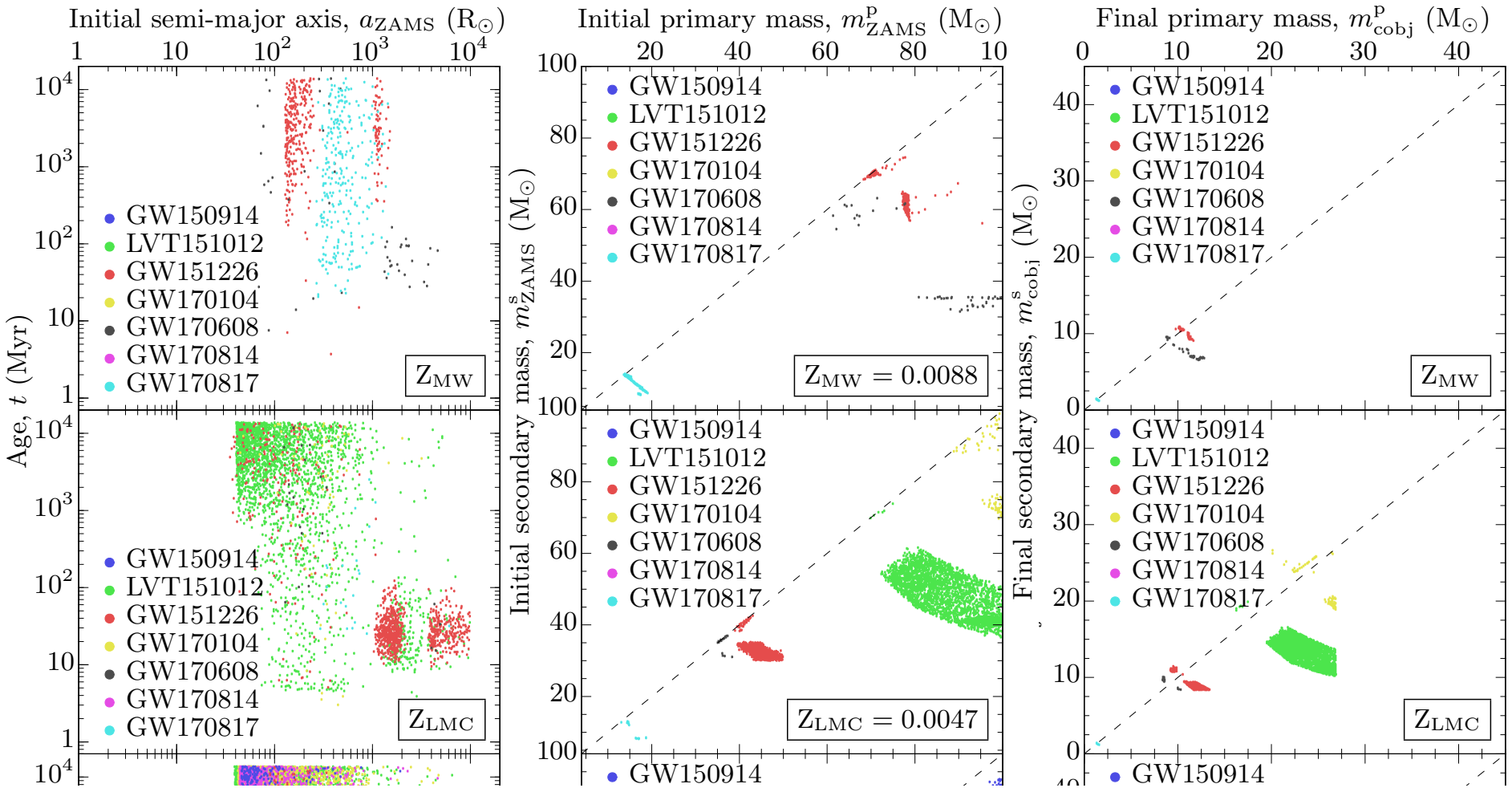

Kruckow et al. (2018)

Merger Rates

Table 8. Our simulated merger-rate densities $\mathcal{R}$ at redshift zero following the two different star-formation history and galaxy-density scaling methods outlined in Dominik et al. (2013) and Abadie et al. (2010), yielding $\mathcal{R}_{z=0}$ and $\mathcal{R}_{\rm cSFR}$, respectively. Using $\langle \mathcal{M}^{2.5} \rangle$, some geometrical factors and assuming a signal-to-noise threshold, $\rho \geq 8$, we calculate the expected LIGO-Virgo detection rates $\mathcal{R}_{\rm D}$ and $\mathcal{R}_{\rm D,cSFR}$ (following equation (3) of Dominik et al. 2015, cf. their table 1). The merger-rate densities and detection rates are calculated for two different metallicity environments ($Z_{\rm MW} = 0.0088$ and $Z_{\rm IZw18} = 0.0002$, top and central panel, respectively) applying our default input parameter settings (Table 2). The bottom panel shows our rates calculated under an "optimistic" setting at MW metallicity to boost the NS-NS merger rate (i.e. applying $\alpha_{\rm IMF} = 2.3$, $\alpha_{\rm RLO} = 0.15$, $\beta_{\rm min} = 0.5$, $\alpha_{\rm CE} = 0.8$ and $\alpha_{\rm TH} = 0.3$). See Section 5.2.4 for a discussion.

$Z_{\rm MW}$	$\langle \mathcal{M}^{2.5} \rangle$	$\mathcal{R}_{z=0}$	$\mathcal{R}_{\rm D}$	$\mathcal{R}_{\rm cSFR}$	$\mathcal{R}_{\rm D,cSFR}$
NS-NS	1.36 $M_\odot^{2.5}$	9.85×10^{0} yr^{-1} Gpc^{-3}	0.28 yr^{-1}	3.47×10^{1} yr^{-1} Gpc^{-3}	0.98 yr^{-1}
NS-BH	20.0 $M_\odot^{2.5}$	0.00×10^{0} yr^{-1} Gpc^{-3}	0.00 yr^{-1}	0.00×10^{0} yr^{-1} Gpc^{-3}	0.00 yr^{-1}
BH-NS	15.7 $M_\odot^{2.5}$	1.80×10^{1} yr^{-1} Gpc^{-3}	5.88 yr^{-1}	4.72×10^{1} yr^{-1} Gpc^{-3}	15.43 yr^{-1}
BH-BH	233 $M_\odot^{2.5}$	6.01×10^{-1} yr^{-1} Gpc^{-3}	2.92 yr^{-1}	3.08×10^{0} yr^{-1} Gpc^{-3}	14.95 yr^{-1}
$Z_{\rm IZw18}$	$\langle \mathcal{M}^{2.5} \rangle$	$\mathcal{R}_{z=0}$	$\mathcal{R}_{\rm D}$	$\mathcal{R}_{\rm cSFR}$	$\mathcal{R}_{\rm D,cSFR}$
NS-NS	1.27 $M_\odot^{2.5}$	1.00×10^{1} yr^{-1} Gpc^{-3}	0.27 yr^{-1}	3.28×10^{1} yr^{-1} Gpc^{-3}	0.87 yr^{-1}
NS-BH	32.3 $M_\odot^{2.5}$	6.61×10^{-3} yr^{-1} Gpc^{-3}	0.00 yr^{-1}	1.55×10^{-2} yr^{-1} Gpc^{-3}	0.01 yr^{-1}
BH-NS	35.5 $M_\odot^{2.5}$	1.54×10^{1} yr^{-1} Gpc^{-3}	11.40 yr^{-1}	5.32×10^{1} yr^{-1} Gpc^{-3}	39.34 yr^{-1}
BH-BH	1720 $M_\odot^{2.5}$	1.68×10^{1} yr^{-1} Gpc^{-3}	603.02 yr^{-1}	3.45×10^{1} yr^{-1} Gpc^{-3}	1235.27 yr^{-1}
optimistic	$\langle \mathcal{M}^{2.5} \rangle$	$\mathcal{R}_{z=0}$	$\mathcal{R}_{\rm D}$	$\mathcal{R}_{\rm cSFR}$	$\mathcal{R}_{\rm D,cSFR}$
NS-NS	1.31 $M_\odot^{2.5}$	7.09×10^{1} yr^{-1} Gpc^{-3}	1.94 yr^{-1}	1.59×10^{2} yr^{-1} Gpc^{-3}	4.37 yr^{-1}
NS-BH	19.4 $M_\odot^{2.5}$	0.00×10^{0} yr^{-1} Gpc^{-3}	0.00 yr^{-1}	0.00×10^{0} yr^{-1} Gpc^{-3}	0.00 yr^{-1}
BH-NS	21.9 $M_\odot^{2.5}$	1.34×10^{1} yr^{-1} Gpc^{-3}	6.11 yr^{-1}	2.44×10^{1} yr^{-1} Gpc^{-3}	11.17 yr^{-1}
BH-BH	275 $M_\odot^{2.5}$	4.34×10^{1} yr^{-1} Gpc^{-3}	248.34 yr^{-1}	1.09×10^{2} yr^{-1} Gpc^{-3}	623.03 yr^{-1}

Table 4. GW merger rates in a MW-like galaxy. The values are based on systems merging within 10^{10} yr. The upper and lower bounds are for systems merging within (10 ± 3.81) Gyr. The binary types indicate the order of the first and second-formed compact objects.

GW merger rates	$Z_{\rm MW} = 0.0088$	$Z_{\rm IZw18} = 0.0002$
NS-NS	$2.98^{+0.15}_{-0.24}\times10^{-6}$ yr^{-1}	$2.82^{+0.16}_{-0.27}\times10^{-6}$ yr^{-1}
NS-BH	$0.00^{+0.00}_{-0.00}\times10^{0}$ yr^{-1}	$1.33^{+0.13}_{-0.22}\times10^{-9}$ yr^{-1}
BH-NS	$4.05^{+0.35}_{-0.59}\times10^{-6}$ yr^{-1}	$4.57^{+0.26}_{-0.37}\times10^{-6}$ yr^{-1}
BH-BH	$2.64^{+0.05}_{-0.07}\times10^{-7}$ yr^{-1}	$2.96^{+0.50}_{-0.55}\times10^{-6}$ yr^{-1}

Kruckow et al. (2018)

- about 3 double neutron stars binaries should merge per Myr in the MW

→ about 1 (to 4) detections per yr at design sensitivity of LIGO

- The merger rate density of 1540^{+3200}_{-1220} yr^{-1} Gpc^{-3} based on one merger probably too high and will change in O3 and O4

Summary and Conclusions

- More accurate treatment of common-envelope evolution, SN kicks depending on binary history, Case BB RLO and more in ComBinE
- Any population synthesis making predictions for NS mergers need to explain the results of pulsar observations (i.e. pulsar masses, orbits)

→ ComBinE reproduces orbits, mass ratios and partly NS-NS masses

→ about 400 active radio pulsars in double NS binaries in the MW galaxy

- All LIGO/Virgo detections reproduced depending on metallicity
- LIGO/Virgo rates are still very uncertain → will decrease in O3 and O4

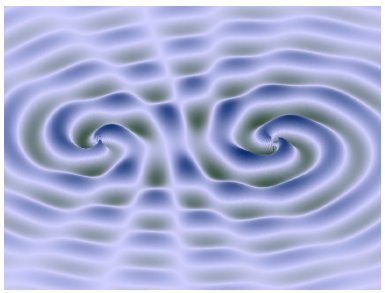

Thanks for your attention!